and North Atlantic and indicate the potential for amplification of decadal-scale variability through interbasin resonance (*42*, *43*). Before the 1970s, variability in poleward heat fluxes and storm tracks in the North Pacific and North Atlantic regions were uncorrelated; more recently, highly correlated behavior has emerged (*44*). Our study documents that the development of such teleconnected variability between these regions is a fundamentally important phenomenon associated with rapid warming, suggesting that such properties may be high-priority targets for detailed monitoring in the future.

REFERENCES AND NOTES

1. R. B. Alley *et al.*, *Nature* **362**, 527–529 (1993).
2. J. P. Steffensen *et al.*, *Science* **321**, 680–684 (2008).
3. W. Dansgaard *et al.*, *Nature* **364**, 218–220 (1993).
4. W. S. Broecker, D. M. Peteet, D. Rind, *Nature* **315**, 21–26 (1985).
5. P. U. Clark *et al.*, *Science* **293**, 283–287 (2001).
6. J. F. McManus, R. Francois, J.-M. Gherardi, L. D. Keigwin, S. Brown-Leger, *Nature* **428**, 834–837 (2004).
7. W. S. Broecker, *Paleoceanography* **13**, 119–121 (1998).
8. J. B. Pedro *et al.*, *Clim. Past* **7**, 671–683 (2011).
9. D. C. Lund, A. C. Mix, *Paleoceanography* **13**, 10–19 (1998).
10. O. A. Saenko, A. Schmittner, A. J. Weaver, *J. Clim.* **17**, 2033–2038 (2004).
11. Y. Okazaki *et al.*, *Science* **329**, 200–204 (2010).
12. A. Timmermann, F. Justino, F.-F. Jin, U. Krebs, H. Goosse, *Clim. Dyn.* **23**, 353–370 (2004).
13. Y. M. Okumura, C. Deser, A. Hu, A. Timmermann, S. P. Xie, *J. Clim.* **22**, 1424–1445 (2009).
14. H. Gebhardt *et al.*, *Paleoceanography* **23**, PA4212 (2008).
15. J. P. Kennett, L. B. Ingram, *Nature* **377**, 510–514 (1995).
16. L. Max *et al.*, *Paleoceanography* **27**, PA3213 (2012).
17. A. C. Mix *et al.*, *Geophys. Monogr.* **112**, 127–148 (1999).
18. M. H. Davies *et al.*, *Paleoceanography* **26**, PA2223 (2011).
19. T. M. Lenton *et al.*, *Proc. Natl. Acad. Sci. U.S.A.* **105**, 1786–1793 (2008).
20. V. Dakos *et al.*, *Proc. Natl. Acad. Sci. U.S.A.* **105**, 14308–14312 (2008).
21. V. Dakos, E. H. van Nes, R. Donangelo, H. Fort, M. Scheffer, *Theor. Ecol.* **3**, 163–174 (2010).
22. M. Scheffer *et al.*, *Science* **338**, 344–348 (2012).
23. J. Bakke *et al.*, *Nat. Geosci.* **2**, 202–205 (2009).
24. T. M. Lenton, V. N. Livina, V. Dakos, M. Scheffer, *Clim. Past.* **8**, 1127–1139 (2012).
25. V. N. Livina, T. M. Lenton, *Geophys. Res. Lett.* **34**, L03712 (2007).
26. S. O. Rasmussen *et al.*, *J. Geophys. Res.* **111**, D06102 (2006).
27. B. E. Caissie, J. Brigham-Grette, K. T. Lawrence, T. D. Herbert, M. S. Cook, *Paleoceanography* **25**, PA1206 (2010).
28. J. A. Barron, L. Heusser, T. Herbert, M. Lyle, *Paleoceanography* **18**, PA1020 (2003).
29. C. Waelbroeck *et al.*, *Nature* **412**, 724–727 (2001).
30. E. Bard, F. Rostek, J. L. Turon, S. Gendreau, *Science* **289**, 1321–1324 (2000).
31. W. Broecker, A. E. Putnam, *Quat. Sci. Rev.* **57**, 17–25 (2012).
32. E. Monnin *et al.*, *Earth Planet. Sci. Lett.* **224**, 45–54 (2004).
33. B. Lemieux-Dudon *et al.*, *Quat. Sci. Rev.* **29**, 8–20 (2010).
34. T. M. Cronin *et al.*, *Quat. Sci. Rev.* **29**, 3415–3429 (2010).
35. H. Asahi, K. Takahashi, *Prog. Oceanogr.* **72**, 343–363 (2007).
36. F. Justino, A. Timmermann, U. Merkel, E. P. Souza, *J. Clim.* **18**, 2826–2846 (2005).
37. F. S. R. Pausata, C. Li, J. J. Wettstein, M. Kageyama, K. H. Nisancioglu, *Clim. Past* **7**, 1089–1101 (2011).
38. D. J. Ullman, A. N. LeGrande, A. E. Carlson, F. S. Anslow, J. M. Licciardi, *Clim. Past* **10**, 487–507 (2014).
39. G. Shaffer, J. Bendtsen, *Nature* **367**, 354–357 (1994).
40. M. H. Davies *et al.*, *Earth Planet. Sci. Lett.* **397**, 57–66 (2014).
41. A. J. Weaver, O. A. Saenko, P. U. Clark, J. X. Mitrovica, *Science* **299**, 1709–1713 (2003).
42. L. Wu, Z. Liu, *J. Clim.* **18**, 331–349 (2005).
43. C. Li, L. Wu, Q. Wang, L. Qu, L. Zhang, *Clim. Dyn.* **32**, 753–765 (2009).
44. E. K. M. Chang, *J. Clim.* **17**, 4230–4244 (2004).
45. A. S. Dyke, in *Quaternary Glaciations: Extent and Chronology*, J. Ehlers, P. L. Gibbard, Eds. (Elsevier, Amsterdam, 2004), pp. 373–424.
46. M. Sarnthein, U. Plaufmann, M. Weinelt, *Paleoceanography* **18**, 1047 (2003).

ACKNOWLEDGMENTS

We thank B. Jensen and D. Froese for the tephra analyses; J. Southon for assistance with radiocarbon samples; A. Ross, J. Padman, and J. McKay of the College of Earth, Ocean and Atmospheric Sciences Stable Isotope Lab; and five anonymous reviewers. This work was supported by NSF grants AGS-0602395 (Project PALEOVAR) and OCE-1204204 to A.C.M., and an NSF graduate research fellowship to S.K.P. The data can be found in the supplementary online materials and at the National Oceanic and Atmospheric Administration Paleoclimate Database.

SUPPLEMENTARY MATERIALS

www.sciencemag.org/content/345/6195/444/suppl/DC1
Materials and Methods
Supplementary Text
Figs. S1 to S11
Tables S1 and S2
References (*47*–*66*)

10 February 2014; accepted 24 June 2014
10.1126/science.1252000

INDUCED EARTHQUAKES

Sharp increase in central Oklahoma seismicity since 2008 induced by massive wastewater injection

K. M. Keranen,[1]* M. Weingarten,[2] G. A. Abers,[3]† B. A. Bekins,[4] S. Ge[2]

Unconventional oil and gas production provides a rapidly growing energy source; however, high-production states in the United States, such as Oklahoma, face sharply rising numbers of earthquakes. Subsurface pressure data required to unequivocally link earthquakes to wastewater injection are rarely accessible. Here we use seismicity and hydrogeological models to show that fluid migration from high-rate disposal wells in Oklahoma is potentially responsible for the largest swarm. Earthquake hypocenters occur within disposal formations and upper basement, between 2- and 5-kilometer depth. The modeled fluid pressure perturbation propagates throughout the same depth range and tracks earthquakes to distances of 35 kilometers, with a triggering threshold of ~0.07 megapascals. Although thousands of disposal wells operate aseismically, four of the highest-rate wells are capable of inducing 20% of 2008 to 2013 central U.S. seismicity.

Seismicity in the United States midcontinent surged beginning in 2008 (*1*), predominantly within regions of active unconventional hydrocarbon production (*2*–*6*). In Arkansas, Texas, Ohio, and near Prague, Oklahoma, recent earthquakes have been linked to wastewater injection (*2*–*7*), although alternative interpretations have been proposed (*1*, *8*). Conclusively distinguishing human-induced earthquakes solely on the basis of seismological data remains challenging.

Seismic swarms within Oklahoma dominate the recent seismicity in the central and eastern United States (*9*), contributing 45% of magnitude (M) 3 and larger earthquakes between 2008 and 2013 (*10*). No other state contributed more than 11%. A single swarm, beginning in 2008 near Jones, Oklahoma, accounts for 20% of seismicity in this region (*10*). East of Jones, the damaging 2011 moment magnitude (M_w) 5.7 earthquake near Prague, Oklahoma, was likely induced by wastewater injection (*2*, *8*, *11*, *12*), the highest magnitude to date. These earthquakes are part of a 40-fold increase in seismicity within Oklahoma during 2008 to 2013 as compared to 1976 to 2007 (Fig. 1, inset A) (*10*). Wastewater disposal volumes have also increased rapidly, nearly doubling in central Oklahoma between 2004 and 2008. Many studies of seismicity near disposal wells rely upon statistical relationships between the relative timing of seismicity, disposal well location, and injected water volume to evaluate a possible causal relationship (*3*–*7*, *13*).

Here we focused on the Jones swarm and compared modeled pore pressure from hydrogeological models to the best-constrained earthquake hypocenters (*14*). Using data from local U.S. Geological Survey NetQuake accelerometers, the Earthscope Transportable Array, and a small local seismic network (fig. S1), we generated a catalog of well-located earthquakes between 2010 and 2013. Event-station distances were predominantly less than 10 km (fig. S2D), and all earthquakes were recorded on at least one seismometer within 20 km of the initial hypocenter. To study pore pressure changes at earthquake hypocenters and the apparent migration in seismicity, we developed a three-dimensional hydrogeological model of pore pressure diffusion from injection wells.

The Jones swarm began within 20 km of high-rate wastewater disposal wells, among the highest rate in Oklahoma, between two regions of fluid injection (Fig. 2). The four high-rate wells are southwest of Jones in southeast Oklahoma City (SE OKC) and dispose of ~4 million barrels per month (*15*) (Fig. 3). The target injection depth is 2.2 to 3.5 km into the Cambrian-Ordovician

[1]Department of Earth and Atmospheric Sciences, Cornell University, Ithaca, NY, USA. [2]Department of Geological Sciences, University of Colorado, Boulder, CO, USA. [3]Lamont-Doherty Earth Observatory of Columbia University, Palisades, NY, USA. [4]U.S. Geological Survey, Menlo Park, CA, USA.
***Corresponding author. E-mail: keranen@cornell.edu** †Present address: Department of Earth and Atmospheric Sciences, Cornell University, Ithaca, NY, USA.

Arbuckle Group (fig. S3), a dolomitized carbonate; one disposal well ends near Precambrian basement. The large disposal wells are within dewatering plays (fig. S4). Dewatering production wells produce substantial wastewater volumes with initially up to 200 times as much water per barrel of oil as conventional production wells (*16*, *17*). The rate of wastewater disposal in central Oklahoma has gradually increased since the mid-1990s (fig. S5), but disposal rates jumped after 2004 as high-rate injection wells began operating, including the first of the SE OKC wells in 2005 (Fig. 3) (*15*). Seismic moment release escalated in the Jones swarm in 2009, concurrent with the initial reported application

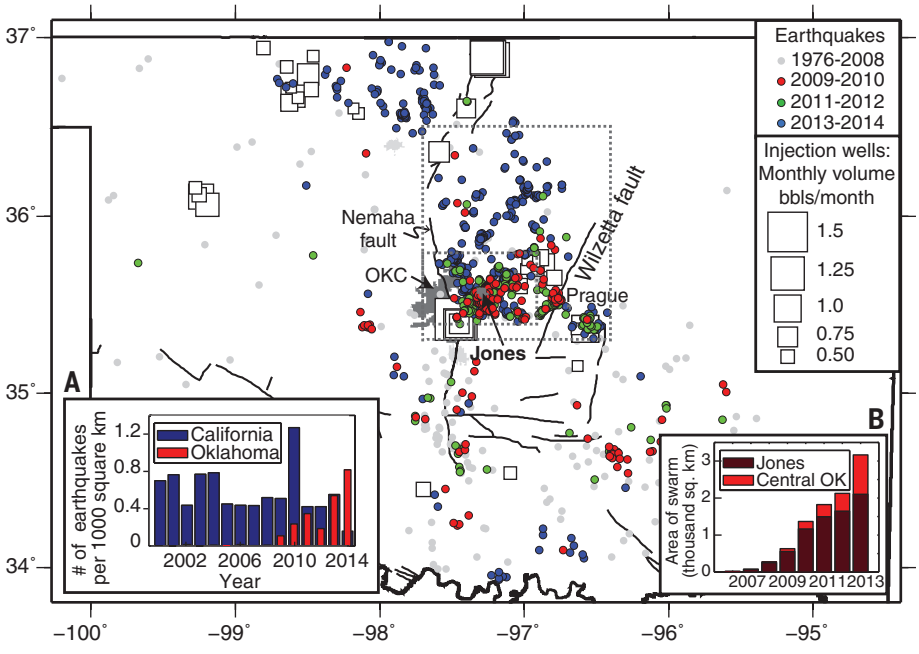

Fig. 1. Earthquakes in Oklahoma between 1976 and 2014. Earthquakes are $M > 1$ from the NEIC catalog (*10*). Black lines are faults (*26*–*28*). Small and large dashed gray boxes outline the areas used for analysis of the Jones swarm and of central Oklahoma, respectively, in inset B. OKC: Oklahoma City. **Inset A:** Comparison of *M*3+ earthquake rate in Oklahoma and California, normalized by area. California is ~2.3 times larger than Oklahoma. 2014 earthquakes are through the first 4 months. **Inset B:** Expanding area of the Jones and the broader central Oklahoma swarms. Regions were divided into 5 km by 5 km grid cells, and any cell with an earthquake was considered part of the swarm. Swarm area per year is inclusive of all prior years.

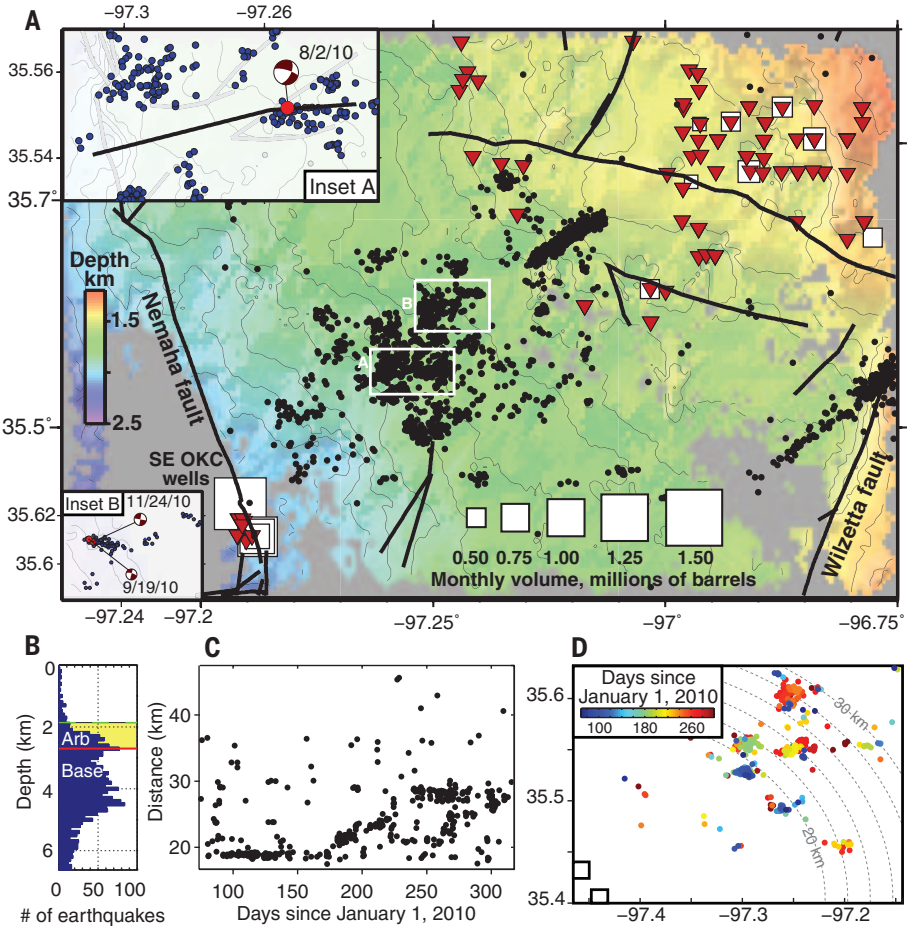

Fig. 2. Earthquake catalog and swarm migration. (**A**) Jones earthquake catalog March 2010 to March 2013 using local stations. Squares are injection wells operating at an average rate ≥ 400,000 barrels per month (*15*, *29*); triangles are high–water production wells. Background color and contours represent depth to the top of the Hunton Group (*15*). The Hunton Group is higher in section than the Arbuckle Group but has more data on formation depth. (**B**) Earthquake depth histogram; earthquakes are dominantly in sediment and upper basement. (**C**) Distance of each March to October 2010 Jones earthquake to the SE OKC disposal wells. The dense region of the swarm increases in distance between days 150 and 250 in 2010. (**D**) Map view of Jones earthquakes during March to October 2010, colored by time. Semicircles are equidistant lines from SE OKC disposal wells. Faults at greater distance from the wells become active at later times. Details of two of these fault planes are shown in insets of Fig. 2A and are discussed in the text.

of positive wellhead pressure at the SE OKC wells (Fig. 3B).

Earthquakes in our catalog primarily nucleated either within the Arbuckle Group or within the upper 2 km of basement, with 22 to 33% above basement (Fig. 2B and fig. S6). Well-constrained earthquake hypocenters from March to October 2010 migrated northeast from the initial swarm centroid near Jones at 0.1 to 0.15 km/day (Fig. 2, C and D), followed by a broad spread in seismicity. Earthquake hypocenters are not diffusely distributed; instead, relocated aftershock sequences of individual earthquakes (*18*) illuminate narrow faults parallel to one plane of calculated focal mechanisms (*19*) (Fig. 2A, insets). An earthquake on 2 August 2010 ruptured a portion of a 7-km-long mapped fault; if the entire fault had ruptured, earthquake scaling laws suggest a maximum magnitude of ~*M*6.0 (*20*). Earthquakes later in 2010 ruptured an unmapped east-southeast– to west-northwest–trending fault, at an oblique angle to the overall northeast-southwest migration direction of the swarm. Although the swarm of seismicity migrates to the northeast parallel to structural dip, the individual faults, as evidenced by earthquake lineations, are not preferentially oriented in this direction.

Our hydrogeological model simulated injection into the Arbuckle Group using reported injection rates at 89 wells within 50 km of the Jones swarm between 1995 and 2012 (*14*). The wells include the four high-rate wells in SE OKC and 85 wells to the northeast of Jones. The model predicts a region of high fluid pressure perturbation spreading radially eastward from the SE OKC wells and a lesser perturbation around the lower-rate wells to the northeast (Fig. 4). The high pore pressure increase occurs within the Arbuckle Group and in the upper 1 to 2 km of the basement in our model; nearly all earthquakes occur within this same depth range (Fig. 2B). The migrating front of the Jones earthquake swarm corresponds closely to the expanding modeled pressure perturbation away from the SE OKC wells, which reaches 25 km from the wells by December 2009 and ~35 km by December 2012. The pore pressure change modeled at each hypocenter indicates a critical threshold of ~0.07 MPa, above which earthquakes are triggered. This threshold is compatible with prior observations that static stress changes of as little as ~0.01 to 0.1 MPa are sufficient to trigger earthquakes when faults are near failure in the ambient stress field (*21*–*23*).

Our results indicate that for modeled diffusivities, ~85% of the pore pressure perturbation is contributed by the four high-rate SE OKC wells. The 85 wells to the northeast contribute ~15% additional pore pressure change at the center of the Jones swarm by the end of 2012 and may contribute to the triggering of earthquakes particularly outside the region affected by the SE OKC wells (fig. S7). The modeled dominance of the SE OKC wells is attributable to their high rate; these wells include one of the largest wells in the state and three closely spaced wells 3.5 km away with a combined monthly volume of ~3 million barrels per month. The only other Oklahoma wells of similar size, in northern Oklahoma (fig. S8), are on the boundary of a second rapidly growing seismic swarm (Fig. 1). The summed rate of this well cluster near SE OKC is higher than previous cases of reported induced seismicity (Fig. 3A), including several times higher than the high-rate disposal wells linked to earthquakes near Dallas–Fort Worth, Texas, and Cleburne, Texas (*5*–*7*). Comprehensive compilations of injection well rates for other high-injection states, including Texas and California, are not yet accessible.

We view the expanding Jones earthquake swarm as a response to regionally increased pore pressure from fluids primarily injected at the SE OKC wells. As the pressure perturbation expanded and encountered faults at various orientations, critically stressed, optimally oriented faults are expected to rupture first (*24*). Additional faults at near-optimal orientations may rupture after further pressure increase (Fig. 4). As fluid pressure continues to

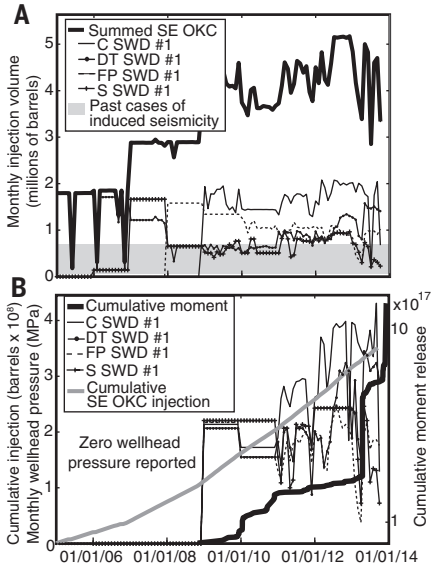

Fig. 3. Fluid injection reported in the four high-rate SE OKC wells. (**A**) Sum and individual monthly injection volumes and (**B**) wellhead pressure and cumulative, summed injected volume (*15*). The DT SWD #1, FP SWD #1, and S SWD #1 wells are in close proximity; the C SWD #1 well is ~3.5 km away. Gray shading denotes injection rates for notable past cases of induced seismicity for reference (table S1). Cumulative seismic moment in (B) is calculated from *M*3+ earthquakes from 2005 to January 2014 (*10*) for earthquakes within the box outlining the Jones swarm in Fig. 1.

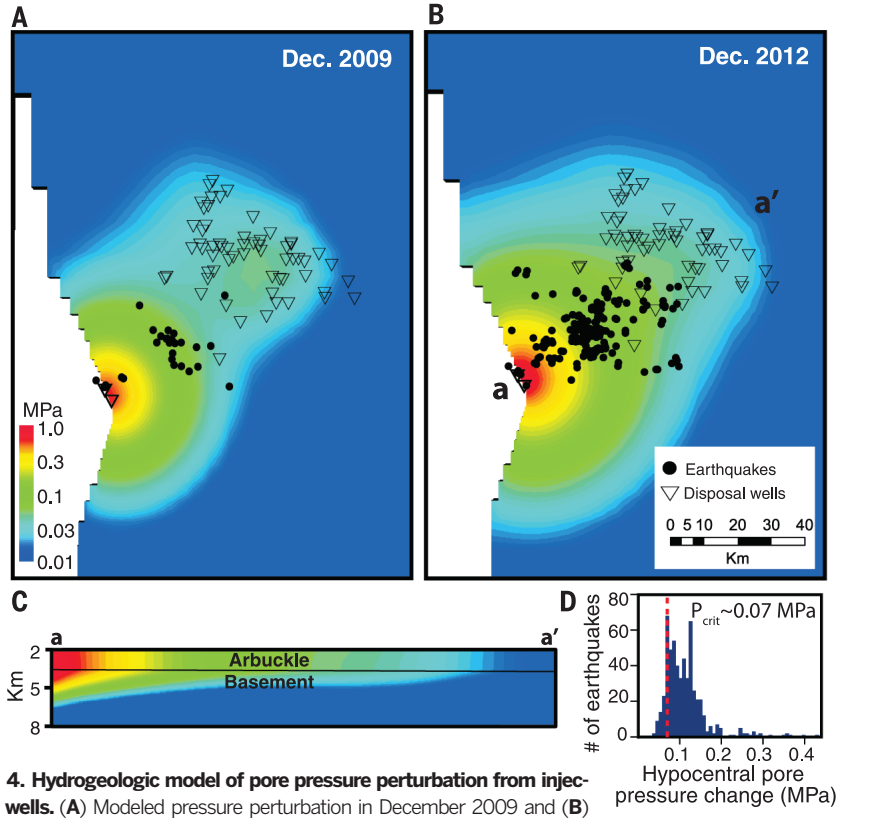

Fig. 4. Hydrogeologic model of pore pressure perturbation from injection wells. (**A**) Modeled pressure perturbation in December 2009 and (**B**) in December 2012 with a hydraulic diffusivity of 2 m^2/s (*14*). The model includes the four high-rate SE OKC wells and 85 wells northeast of the Jones swarm near the West Carney field. The modeled pressure perturbation is dominated by fluid injected at the high-rate SE OKC wells. Earthquakes are plotted from 2008 to 2009 (A) and 2008 to 2012 (B) (*10*). (**C**) Vertical cross section through model results. Pore pressure rises in the Arbuckle Group and uppermost basement. (**D**) Pore pressure increase at the hypocenter of each earthquake in our local catalog. A pore pressure increase of ~0.07 MPa is the modeled triggering threshold. Modeled pore pressure rises throughout much of the swarm area for hydraulic diffusivity between 1 and 4 m^2/s (fig. S7).

propagate away from the wells and disturbs a larger and larger volume, the probability increases that fluid pressure will encounter a larger fault and induce a larger-magnitude earthquake. The absence of earthquakes in regions above the critical pressure threshold may result from either a lack of faults or lack of well-oriented, critically stressed faults. Alternatively, fluid flow may preferentially migrate along bedding structure (Fig. 2A).

Though seven earthquakes were recorded in 2006 to 2009 near the base of the SE OKC wellbores (*10*), the main swarm began ~15 km to the northeast (fig. S9), despite the high modeled pressure perturbation near the wells. Earthquakes in 2009 primarily occurred, within location uncertainty, near injection wells or on the nearest known faults to the northeast of the wells (fig. S9). Focal mechanisms near the swarm onset indicate fault planes at orientations favorable to failure (*19*) (Fig. 2, inset B). Faults subparallel to the north-northwest–south-southeast–trending Nemaha fault would not be well oriented for failure in the regional ~N70E stress regime (*25*) and would require substantially larger pressure increase to fail. Recent earthquakes near the fault may be evidence for continued pressure increase. This 50-km-long segment of the Nemaha fault is capable of hosting a *M*7 earthquake based on earthquake scaling laws (*20*), and the fault zone continues for hundreds of kilometers. The increasing proximity of the earthquake swarm to the Nemaha fault presents a potential hazard for the Oklahoma City metropolitan area.

Our earthquake relocations and pore pressure models indicate that four high-rate disposal wells are capable of increasing pore pressure above the reported triggering threshold (*21*–*23*) throughout the Jones swarm and thus are capable of triggering ~20% of 2008 to 2013 central and eastern U.S. seismicity. Nearly 45% of this region's seismicity, and currently nearly 15 $M > 3$ earthquakes per week, may be linked to disposal of fluids generated during Oklahoma dewatering and after hydraulic fracturing, as recent Oklahoma seismicity dominantly occurs within seismic swarms in the Arbuckle Group, Hunton Group, and Mississippi Lime dewatering plays. The injection-linked seismicity near Jones occurs up to 35 km away from the disposal wells, much further than previously considered in existing criteria for induced seismicity (*13*). Modern, very high-rate injection wells can therefore affect regional seismicity and increase seismic hazard. Regular measurements of reservoir pressure at a range of distances and azimuths from high-rate disposal wells could verify our model and potentially provide early indication of seismic vulnerability.

REFERENCES AND NOTES

1. W. L. Ellsworth, *Science* **341**, 1225942 (2013).
2. K. Keranen, H. Savage, G. Abers, E. Cochran, *Geology* **41**, 699–702 (2013).
3. W.-Y., *J. Geophys. Res.* **118**, 3506–3518 (2013).
4. S. Horton, *Seismol. Res. Lett.* **83**, 250–260 (2012).
5. C. Frohlich, C. Hayward, B. Stump, E. Potter, *Bull. Seismol. Soc. Am.* **101**, 327–340 (2011).
6. A. H. Justinic, B. Stump, C. Hayward, C. Frohlich, *Bull. Seismol. Soc. Am.* **103**, 3083–3093 (2013).
7. C. Frohlich, *Proc. Natl. Acad. Sci. U.S.A.* **109**, 13934–13938 (2012).
8. A. McGarr, *J. Geophys. Res.* **119**, 1008–1019 (2014).
9. The Central and Eastern United States is considered the portion of the contiguous United States east of 109°W.
10. ANSS catalog, United States Geological Survey, http://earthquake.usgs.gov/earthquakes/search/, accessed 4/1/2014.
11. N. J. van der Elst, H. M. Savage, K. M. Keranen, G. A. Abers, *Science* **341**, 164–167 (2013).
12. D. F. Sumy, E. S. Cochran, K. M. Keranen, M. Wei, G. A. Abers, *J. Geophys. Res.* **119**, 1904–1923 (2014).
13. S. D. Davis, C. Frohlich, *Seismol. Res. Lett.* **64**, 207–224 (1993).
14. Information on materials and methods is available on *Science* Online.
15. Oklahoma Corporation Commission Imaging Web Application, http://imaging.occeweb.com/
16. D. Chernicky, *World Oil* (2000); www.worldoil.com/September-2000-Major-reserve-increase-obtained-by-dewatering-high-water-saturation-reservoirs.html.
17. K. E. Murray, *Environ. Sci. Technol.* **47**, 4918–4925 (2013).
18. F. Waldhauser, W. L. Ellsworth, *Bull. Seismol. Soc. Am.* **90**, 1353–1368 (2000).
19. A. A. Holland, *Seismol. Res. Lett.* **84**, 876–890 (2013).
20. D. L. Wells, K. J. Coppersmith, *Bull. Seismol. Soc. Am.* **84**, 974–1002 (1994).
21. P. A. Reasenberg, R. W. Simpson, *Science* **255**, 1687–1690 (1992).
22. L. Seeber, J. G. Armbruster, *Nature* **407**, 69–72 (2000).
23. R. Stein, *Nature* **402**, 605–609 (1999).
24. M. D. Zoback, J. Townend, B. Grollimund, *Int. Geol. Rev.* **44**, 383–401 (2002).
25. M. L. Zoback, *J. Geophys. Res.* **97**, 11703–11728 (1992).
26. K. V. Luza, J. E. Lawson, *Oklahoma Geological Survey Spec. Pub.* **81-3**, 1–67 (1981).
27. S. P. Gay, *Shale Shaker* **54**, 39–49 (2003).
28. L. E. Gatewood, in *Geology of Giant Petroleum Fields*, AAPG Memoir **14**, M. T. Halbouty, Ed. (American Association of Petroleum Geologists Tulsa, OK, 1970).
29. Monthly average volume was calculated by using reported volumes for any month with nonzero volume in data available from 1995 through 2012 (*15*). Injection rates over 90% larger than the median monthly value in a given year for each well were removed from calculations to remove data entry errors.

ACKNOWLEDGMENTS

This research benefited from discussion with E. Cochran, W. Ellsworth, and participants in a U.S. Geological Survey (USGS) Powell Center Working Group on Understanding Fluid Injection Induced Seismicity (M.W., B.A.B., and S.G. are part of this group). C. Hogan identified many *P* and *S* phases. K.M.K was partially supported by USGS National Earthquake Hazards Reduction Program (NEHRP) grant G13AP00025, M.W. was partially supported by the USGS Powell Center grant G13AC00023, and G.A.A. was partially supported by NEHRP grant G13AP00024. This project used seismic data from EarthScope's Transportable Array, a facility funded by the National Science Foundation. Seismic waveforms are from the Incorporated Research Institutions for Seismology Data Management Center and the USGS CWB Query. Well data are from the Oklahoma Corporation Commission and the Oklahoma Geological Survey. Lists of wells and the local earthquake catalog are available as supplementary materials on *Science* Online.

SUPPLEMENTARY MATERIALS

www.sciencemag.org/content/345/6195/448/suppl/DC1
Materials and Methods
Figs. S1 to S10
Tables S1 to S9
References (*30*–*41*)

8 May 2014; accepted 24 June 2014
Published online 3 July 2014;
10.1126/science.1255802

DINOSAUR EVOLUTION

A Jurassic ornithischian dinosaur from Siberia with both feathers and scales

Pascal Godefroit,[1]* Sofia M. Sinitsa,[2] Danielle Dhouailly,[3] Yuri L. Bolotsky,[4] Alexander V. Sizov,[5] Maria E. McNamara,[6,7] Michael J. Benton,[7] Paul Spagna[1]

Middle Jurassic to Early Cretaceous deposits from northeastern China have yielded varied theropod dinosaurs bearing feathers. Filamentous integumentary structures have also been described in ornithischian dinosaurs, but whether these filaments can be regarded as part of the evolutionary lineage toward feathers remains controversial. Here we describe a new basal neornithischian dinosaur from the Jurassic of Siberia with small scales around the distal hindlimb, larger imbricated scales around the tail, monofilaments around the head and the thorax, and more complex featherlike structures around the humerus, the femur, and the tibia. The discovery of these branched integumentary structures outside theropods suggests that featherlike structures coexisted with scales and were potentially widespread among the entire dinosaur clade; feathers may thus have been present in the earliest dinosaurs.

The origin of birds is one of the most-studied diversification events in the history of life. Principal debates relate to the origin of key avian features such as wings, feathers, and flight (*1*–*9*). Numerous finds from China have revealed that diverse theropods possessed feathers and various degrees of flight capability (*4*–*9*). The identification of melanosomes in non-avian theropods (*10*, *11*) confirms that fully birdlike feathers originated within Theropoda at least 50 million years before *Archaeopteryx*.

But were feathers more widespread among dinosaurs? Quill-like structures have been reported in the ornithischians *Psittacosaurus* (*12*) and *Tianyulong* (*13*), but whether these were true feathers, or some other epidermal appendage, is unclear. Bristlelike epidermal appendages occur in pterosaurs, some early theropods (*14*), and extant mammals ("hairs"), and so the *Psittacosaurus*

[1]Directorate 'Earth and History of Life,' Royal Belgian Institute of Natural Sciences, Rue Vautier 29, B-1000 Brussels, Belgium. [2]Institute of Natural Resources, Ecology and Cryology, 26 Butin Street, 672 014 Chita, Russia. [3]UJF-CNRS FRE 3405, AGIM, Université Joseph Fourier, Site Santé, 38 706 La Tronche, France. [4]Institute of Geology and Nature Management, FEB RAS, 1 Relochny Street 675 000, Blagoveschensk, Russia. [5]Institute of the Earth Crust, SB RAS, 128 Lermontov Street, Irkutsk, 664 033 Irkutsk, Russia. [6]School of Biological, Earth and Environmental Science, University College Cork, Cork, Ireland. [7]School of Earth Sciences, University of Bristol, Bristol BS8 1RJ, UK.
*Corresponding author. E-mail: pascal.godefroit@naturalsciences.be

Sharp increase in central Oklahoma seismicity since 2008 induced by massive wastewater injection

K. M. Keranen, M. Weingarten, G. A. Abers, B. A. Bekins and S. Ge

Science **345** (6195), 448-451.
DOI: 10.1126/science.1255802originally published online July 3, 2014

Wastewater disposal linked to earthquakes

The number of earthquakes is increasing in regions with active unconventional oil and gas wells, where water pumped at high pressure breaks open rock containing natural gas, leaving behind wastewater in need of disposing. Keranen *et al.* show that the steep rise in earthquakes in Oklahoma, USA, is likely caused by fluid migration from wastewater disposal wells. Twenty percent of the earthquakes in the central United States could be attributed to just four of the wells. Injected fluids in high-volume wells triggered earthquakes over 30 km away.

Science, this issue p. 448